185

[4]

AN ANALYSIS OF THE GROUNDWATER RESOURCES OF TONGATAPU ISLAND, KINGDOM OF TONGA

BRUCE HUNT

Department of Civil Engineering, University of Canterbury, Christchurch (New Zealand)

ABSTRACT

Hunt, B., 1979. An analysis of the groundwater resources of Tongatapu Island, Kingdom of Tonga. J. Hydrol., 40: 185—196.

An analysis is made of the groundwater resources of Tongatapu Island. The Ghyben-Herzberg approximation is used to estimate thicknesses of a fresh-water lens floating on seawater. Finite-difference calculations are used to estimate rainfall recharge rates, and calculations are made to investigate the dispersion of chloride ions across the fresh-water—salt-water interface. These calculations suggest that artificial recharge might be a useful device to control chloride concentrations in the fresh-water aquifer.

INTRODUCTION

Tongatapu Island is the largest of a group of islands that form the Kingdom of Tonga in the South Pacific Ocean. The island has an area of 245 km², a population of 61,000 people and an average rainfall of 1,700 mm/yr. The geological structure of the island consists of up to 5 m of topsoil overlying a very porous coral limestone that extends to a depth of about 140 m below sea level. No rivers, lakes or reservoirs exist on the island, so that groundwater and rainfall caught on building roofs are the only sources of fresh water. The groundwater is recharged by rainfall and occurs as a fresh-water lens floating on top of denser seawater beneath the island. Water is abstracted, for the most part, from relatively shallow hand-dug wells, and measurements show that chloride contents of this water have increased with increased ground-water usage. The following work is an attempt to add to an understanding of the groundwater resources of Tongatapu Island.

MEASURED PIEZOMETRIC CONTOURS

Table I shows water level measurements, in metres above mean sea level (MSL), taken by the Tonga Water Board in 39 wells on Tongatapu Island. These data have been used to construct the piezometric contour map shown

TABLE I

Water level heights, Cl⁻ ion concentrations and calculated values of parameter ϵ for 39 wells on Tongatapu Island

Well No.	h (m)	$c(0)$ (ppm)	$\epsilon = PB/\sigma D$	Well No.	h (m)	$c(0)$ (ppm)	$\epsilon = PB/\sigma D$
1	0.203	130	7.5	21	0.406	62	8.8
2	0.267	80	8.5	22	0.406	40	9.5
3	0.445	40	9.5	23	0.203	235	6.6
4	0.457	86	8.2	24	0.203	100	8.0
5	0.495	32	10.0	25	0.191	200	6.7
6	0.457	66	8.6	26	0.406	45	9.3
7	0.483	49	9.2	27	0.229	133	7.5
8	0.483	97	8.0	28	0.229	369	5.8
9	0.381	154	7.3	29	0.305	160	7.2
10	0.229	218	6.8	30	0.203	235	6.6
11	0.318	416	5.6	31	0.229	558	5.0
12	0.191	997	4.0	32	0.254	101	8.0
13	0.279	146	7.4	33	0.203	490	5.2
14	0.483	94	8.1	34	0.229	212	6.7
15	0.279	85	8.3	35	0.559	20	10.8
16	0.356	100	8.0	36	0.381	30	10.0
17	0.381	137	7.5	37	0.254	70	8.5
18	0.343	78	8.5	38	0.216	149	7.4
19	0.229	90	8.2	39	0.229	—	—
20	0.229	157	7.2				

in Fig. 1, which also shows the location of the 39 observation wells. The Ghyben-Herzberg approximation, as explained by Bear (1972), states that the interface between fresh-water and salt-water lies below MSL a distance equal to $h/(S-1)$, in which h = free surface elevation above MSL and S = (seawater density)/(fresh-water density), where both densities are taken at the same temperature. Thus, each piezometric contour in Fig. 1 also represents a contour of constant elevation upon the fresh-water—salt-water interface. A value of $S = 1.025$ was used to calculate the elevation of these contours below MSL. These elevations are shown in parentheses below each piezometric contour elevation in Fig. 1, so that the difference of each pair of elevations at any point gives the total thickness of the fresh-water lens. In this approximation, the fresh-water lens is assumed to have a zero thickness at MSL along the coast. A comparison of the computed interface location with some results of a geoelectric survey made by Forbes (1977) is shown in Fig. 2 and suggests that values for the lens thicknesses in Fig. 1 are reasonable.

GROUNDWATER RECHARGE CALCULATIONS

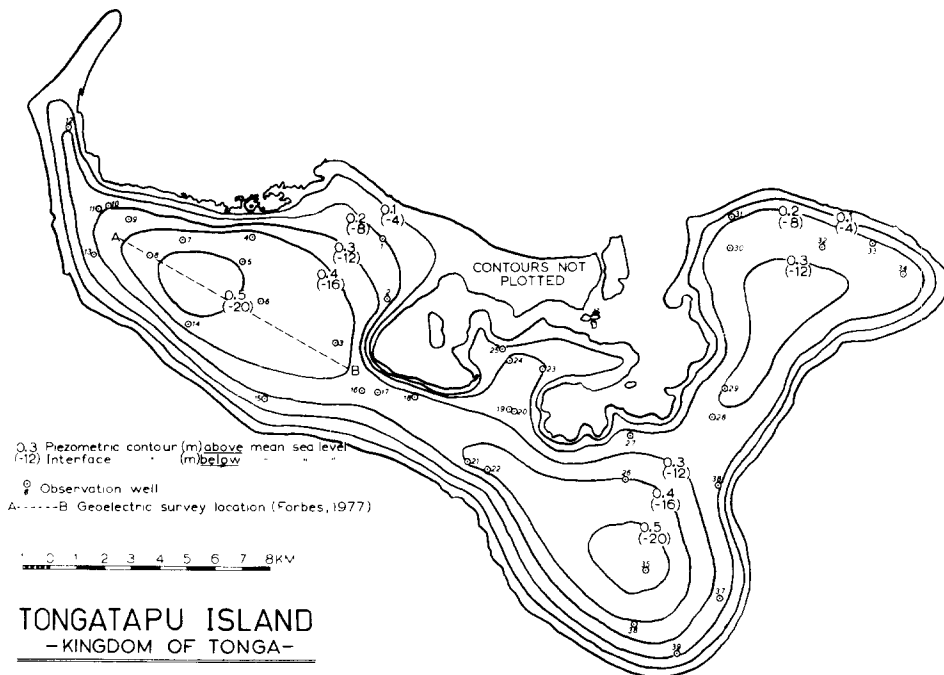The assumption of steady flow and the Dupuit approximation of a hydro-

Fig. 1. Measured piezometric contours, observation well locations and calculated interface contours.

static pressure distribution in the vertical direction lead to the equation (Bear, 1972):

$$\frac{\partial}{\partial x}\left(KB\,\frac{\partial h}{\partial x}\right) + \frac{\partial}{\partial y}\left(KB\,\frac{\partial h}{\partial y}\right) = -P \tag{1}$$

in which h = piezometric head = free surface elevation above MSL; K = coefficient of permeability; B = saturated thickness of the fresh-water lens; P = vertical rainfall discharge velocity (flow rate per unit area); and x, y = horizontal Cartesian coordinates. The Ghyben-Herzberg approximation (Bear, 1972) gives:

$$B = Sh/(S-1) \tag{2}$$

in which S = specific gravity of seawater. Combining eqs. 1 and 2 and assuming that K is constant gives the Poisson equation:

$$\frac{\partial^2(h^2)}{\partial x^2} + \frac{\partial^2(h^2)}{\partial y^2} = -2\left(\frac{S-1}{S}\right)\frac{P}{K} \tag{3}$$

The boundary condition for this problem is:

$$h^2 = 0 \tag{4}$$

along the island edges.

Eqs. 3 and 4, which are linear in h^2, were solved numerically with finite-difference techniques similar to those described by Smith (1965). The island geometry was approximated with a grid containing 293 nodes spaced at 1 km in both the x- and y-directions, as shown in Fig. 3, and eq. 3 was replaced with a second-order central-difference approximation. The variable P/K was taken as a piecewise constant function over the different subregions of the island shown in Fig. 4. Eqs. 3 and 4 suggest that, to a very close approximation over each subregion:

$$h^2 \propto P/K \tag{5}$$

Thus, eq. 5 was used to adjust values of P/K until satisfactory agreement was obtained between the computed piezometric contours, shown in Fig. 3, and the measured piezometric contours, shown in Fig. 1. The corresponding values for P/K are shown in Fig. 4 for each subregion.

Values of P/K in Fig. 4 all have an order of magnitude of 10^{-6}. Differences between values for the various subregions occur as the result of changes in both rainfall recharge and well abstractions, since a more careful definition of P is the difference between rates of rainfall recharge and well abstractions. The exact distribution of well abstractions is unknown at present, although Forbes (1977) estimates total abstractions on the island to be 95,470 m³/month. This value, when divided by the island area of 245 km², gives an average abstraction rate of 0.39 mm/month, which is very small when compared with an average rainfall of 141.7 mm/month. On the other hand, this comparison would be misleading if well abstractions are not distributed uniformly over the island.

A pump test carried out by Waterhouse (1976) measured an equilibrium drawdown of 0.0127 m in an observation well located 3.048 m from the pumped well. The flow rate from the pumped well was 0.273 m³/min, and
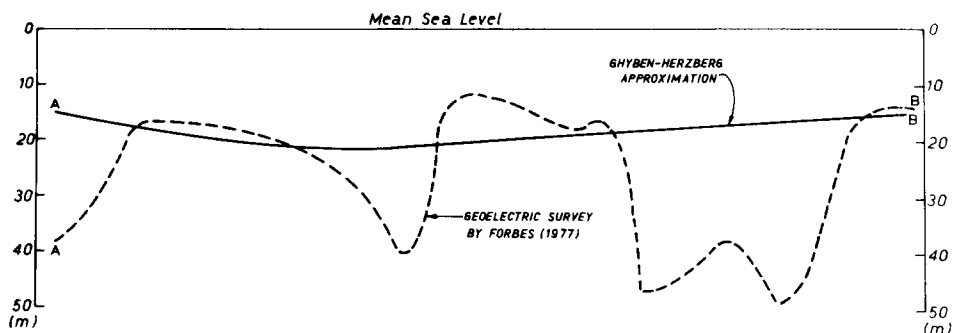

Fig. 2. Interface locations along line AB in Fig. 1 estimated by the Ghyben-Herzberg approximation and by a geoelectric survey.
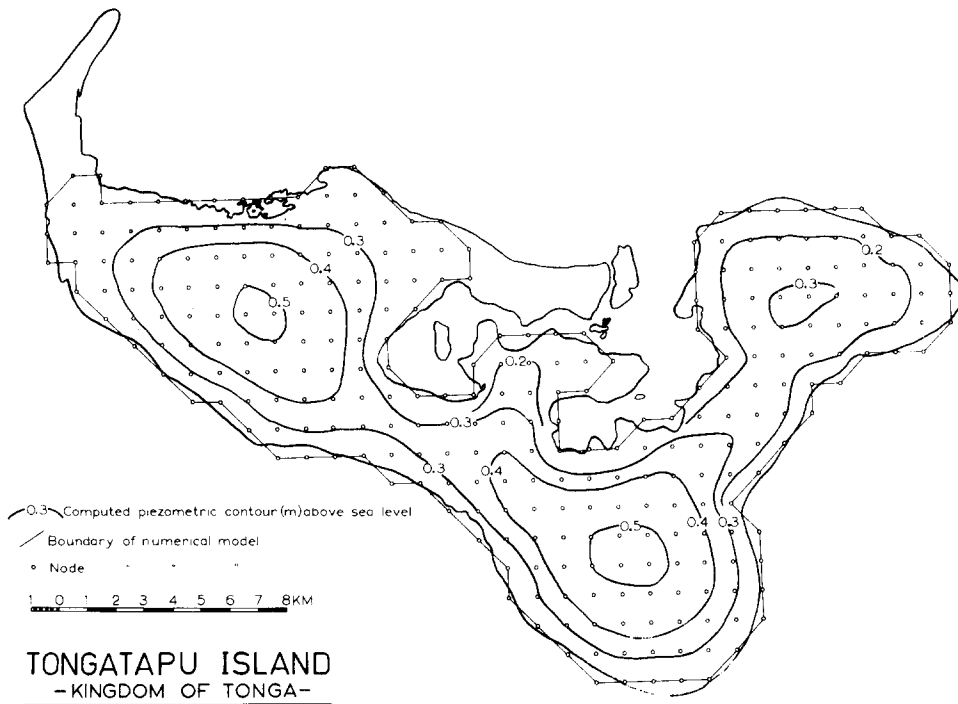
Fig. 3. Finite-difference mesh geometry and calculated piezometric contours.

the pumped well and observation well both penetrated a distance of 3.82 m into an estimated aquifer thickness of 16.4 m. An approximate mathematical solution to this problem can be obtained by distributing sinks along the centreline of the pumped well and its "image" above the free surface. This gives:

$$h = -\frac{Q}{4\pi KL} \int_{-L}^{L} \frac{d\xi}{[r^2 + (z-\xi)^2]^{1/2}} = -\frac{Q}{4\pi KL} \ln \left[\frac{\left(\frac{L+z}{r}\right)^2 + 1\right)^{1/2} + \left(\frac{L+z}{r}\right)}{\left\{\left(\frac{L+z}{r}\right)^2 + 1\right\}^{1/2} - \left(\frac{L-z}{r}\right)} \right] \quad (6)$$

in which Q = flow rate from the pumped well; L = penetration depth of the pumped well; and r and z = polar coordinates of a point on the centreline of the observation well. The values of these variables that were measured by Waterhouse were substituted into eq. 6 to obtain:

$$K = 1.5 \text{ cm/s} \quad (7)$$

This relatively large value of K, which is near the top end of the range given by Harr (1962) as typical for coarse, clean sands, is due to the extremely porous nature of the coral limestone. It can be used with the values of P/K given in Fig. 4 to estimate P. The results are shown in Table II, which indicate

that about 25—30% of the total rainfall (141.7 mm/month) percolates through to the groundwater table over much of the island.

TABLE II

Values of P/K used to calculate recharge rates

P/K ($\times 10^{-6}$)	P (mm/month)	Recharge rate (%)
0.32	12.4	8.8
0.59	22.9	16.2
0.90	35.0	24.7
1.05	40.8	28.8
1.06	41.2	29.1
1.46	56.8	40.1

GROUNDWATER QUALITY CALCULATIONS

The steady-state dispersion of salt across the interface is governed by the following dispersion equation (Bear, 1972):

$$\frac{\partial}{\partial x}\left(D_{xx}\frac{\partial c}{\partial x} + D_{xy}\frac{\partial c}{\partial y} + D_{xz}\frac{\partial c}{\partial z}\right) + \frac{\partial}{\partial y}\left(D_{yx}\frac{\partial c}{\partial x} + D_{yy}\frac{\partial c}{\partial y} + D_{yz}\frac{\partial c}{\partial z}\right) +$$

$$\frac{\partial}{\partial z}\left(D_{zx}\frac{\partial c}{\partial x} + D_{zy}\frac{\partial c}{\partial y} + D_{zz}\frac{\partial c}{\partial z}\right) = \frac{u}{\sigma}\frac{\partial c}{\partial x} + \frac{v}{\sigma}\frac{\partial c}{\partial y} + \frac{w}{\sigma}\frac{\partial c}{\partial z} \qquad (8)$$

in which σ = porosity; u, v and w = flux density components; and D_{ij} = components of the dispersion tensor. The dispersion tensor components depend, in general, upon the velocity magnitude $(u^2 + v^2 + w^2)^{1/2}/\sigma$.

A boundary layer approximation, which applies in this problem since the thickness of the fresh-water lens is much smaller than the lateral dimensions of the lens, suggests that the last term on the left-hand side of eq. 8 makes the dominant contribution to the dispersive terms. The relative magnitude of convective terms on the right-hand side of eq. 8 can be estimated from numbers

TABLE III

Relative magnitude of convective terms in eq. 8

Term	Order of magnitude
u/K, v/K	10^{-4}
w/K	10^{-6}
$\partial c/\partial x$, $\partial c/\partial y$ (ppm/m)	10^{-1}
$\partial c/\partial z$ (ppm/m)	10^3

given in Table III. The values in Table III suggest that the last term on the right-hand side of eq. 8 is about two orders of magnitude larger than the other two convective terms. Furthermore, values of the dispersion tensor components are, to a first approximation, functions of the horizontal velocity, which is two orders of magnitude larger than the vertical flux density, w. Thus, this application allows eq. 8 to be approximated with:

$$D \frac{\partial^2 c}{\partial z^2} = \frac{w}{\sigma} \frac{\partial c}{\partial z} \tag{9}$$

in which D is a lateral dispersion coefficient determined by the magnitude of the horizontal velocity and, therefore, is independent of z. Polubarinova-Kochina (1972) shows how the Dupuit approximation can be used to obtain a first approximation to the vertical velocity component as a linear function of z. Thus, if z is measured from the free surface and is positive in the upward direction, it is reasonable to approximate w in eq. 9 with:

$$w = -P(1 + z/B) \tag{10}$$

in which B = fresh-water lense thickness given by eq. 2. The boundary condition at $z = -B$ will be taken as:

$$c = c_s \tag{11}$$

in which c_s = Cl^- concentration of seawater = 19,000 ppm. The boundary condition on the free surface, $z = 0$, is:

$$D(\partial c/\partial z) + (P/\sigma)c = 0 \tag{12}$$

Eq. 12 has the physical meaning that the free surface acts as a barrier to the dispersion process. Solution of eqs. 9—12 gives:

$$c(z)/c_s = 1 - \frac{(\pi\epsilon/2)^{1/2} \exp(\epsilon/2) \, \text{erf} \, [(1 + z/B)(\epsilon/2)^{1/2}]}{1 + (\pi\epsilon/2)^{1/2} \exp(\epsilon/2) \, \text{erf}[(\epsilon/2)^{1/2}]} \tag{13}$$

in which:

$$\epsilon \equiv PB/\sigma D \tag{14}$$

The dimensionless number, ϵ, is analogous to the Peclet number of heat transfer and can be given the physical interpretation of the ratio of a downward rainfall recharge velocity to an upward dispersive velocity of the Cl^- ions.

A plot of eq. 13, for five different values of ϵ, is shown in Fig. 5. This plot shows that the Cl^- concentration is everywhere equal to that of seawater for $\epsilon = 0$ and that measurable Cl^- concentrations become confined to a smaller and smaller region near the interface as ϵ increases from 0 to a large positive number. Since ϵ increases with P, it is seen that an increase in rainfall recharge decreases Cl^- concentrations and a decrease in P either as the result of less rain or larger well abstractions, causes an increase in $c(z)/c_s$ at any fixed point in the fresh-water lens.
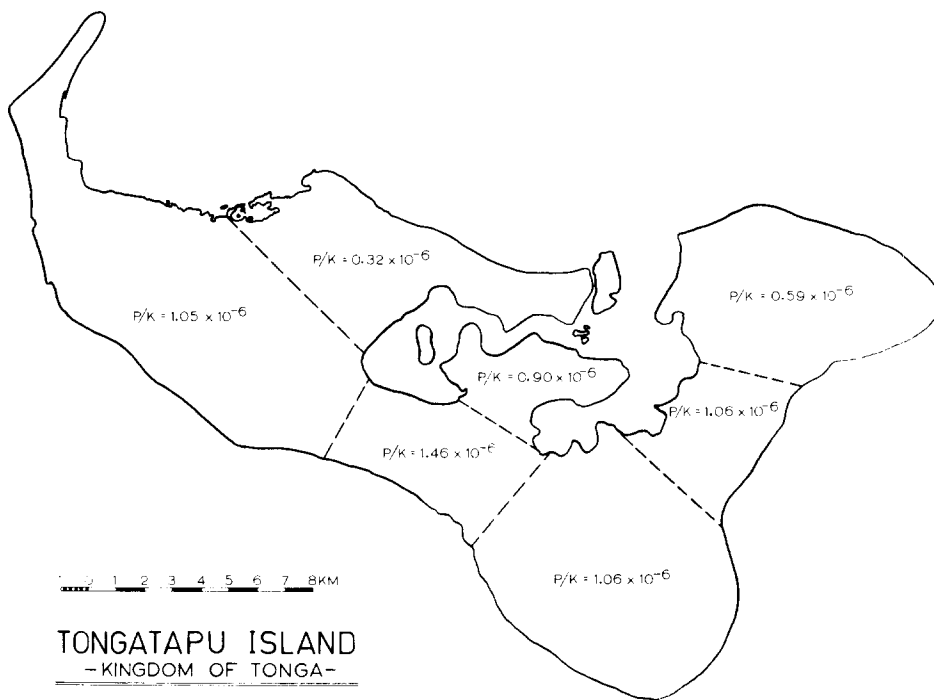
Fig. 4. Values of P/K used to calculate the piezometric contours shown in Fig. 3.

Values of $c(0)$ that were measured by the Tonga Water Board in February of 1971 are shown in Table I. These values were substituted into eq. 13 to calculate ϵ, values of which are also given in Table I. A contour map of ϵ, drawn from the values given in Table I, is shown in Fig. 6. This contour map shows that the higher values of ϵ (and, therefore, the lower values of $c(0)/c_s$) occur near central portions of the island where piezometric contours attain their maximum elevations.

Since $c(0) = f(\epsilon)$, it is possible to prepare a plot of $c_1(0)$ vs. ϵ_2/ϵ_1 for constant values of $c_2(0)/c_1(0)$. [The subscripts are defined by $c_1(0) \equiv f(\epsilon_1)$ and $c_2(0) \equiv f(\epsilon_2)$, and a value of 19,000 ppm has been used for c_s.] This plot is shown in Fig. 7. The value of Fig. 7 is increased considerably by noting that eqs. 2, 5 and 14, and the fact that D is often approximated by the product of the horizontal velocity component with a constant dispersivity (thus, $D \propto p^{1/2}$ by eq. 5) gives the approximation:

$$\epsilon_2/\epsilon_1 \cong P_2/P_1 \cong h_2^2/h_1^2 \tag{15}$$

Thus, Fig. 7 can be used to estimate the change in $c(0)$ that will occur as the result of a change in either P or h.

As an example of the use of Fig. 7, assume that either artificial recharge or decreased well abstractions allow P to be increased by 7% in a region that
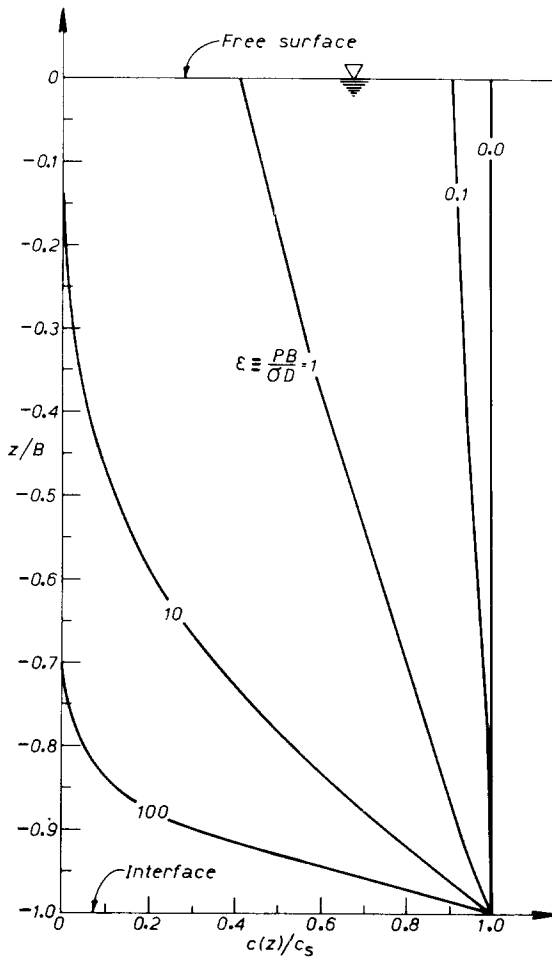
Fig. 5. Chloride concentrations calculated from eq. 13.

initially has a concentration of 200 ppm. Then $c_1(0) = 200$ ppm, eq. 15 gives $\epsilon_2/\epsilon_1 \cong 1.07$ and Fig. 7 gives $c_2(0)/c_1(0) = 0.75$. Thus, the Cl$^-$ concentration will be decreased by 25% to $0.75 \times 200 = 150$ ppm.

For a second example, assume that a groundwater model has been used to predict that future well abstractions will decrease h by 5% in a region that initially has free-surface concentrations of 200 ppm. Then $c_1(0) = 200$ ppm, eq. 15 gives $\epsilon_2/\epsilon_1 \approx (0.95)^2 = 0.90$ and Fig. 7 gives $c_2(0)/c_1(0) = 1.45$. Thus, Cl$^-$ concentrations will be increased 45% to $1.45 \times 200 = 290$ ppm. As a matter of interest, the World Health Organisation (Fried, 1975) gives values of 200 and 600 ppm for "maximum proposed" and "maximum admissible" Cl$^-$ concentrations, respectively.

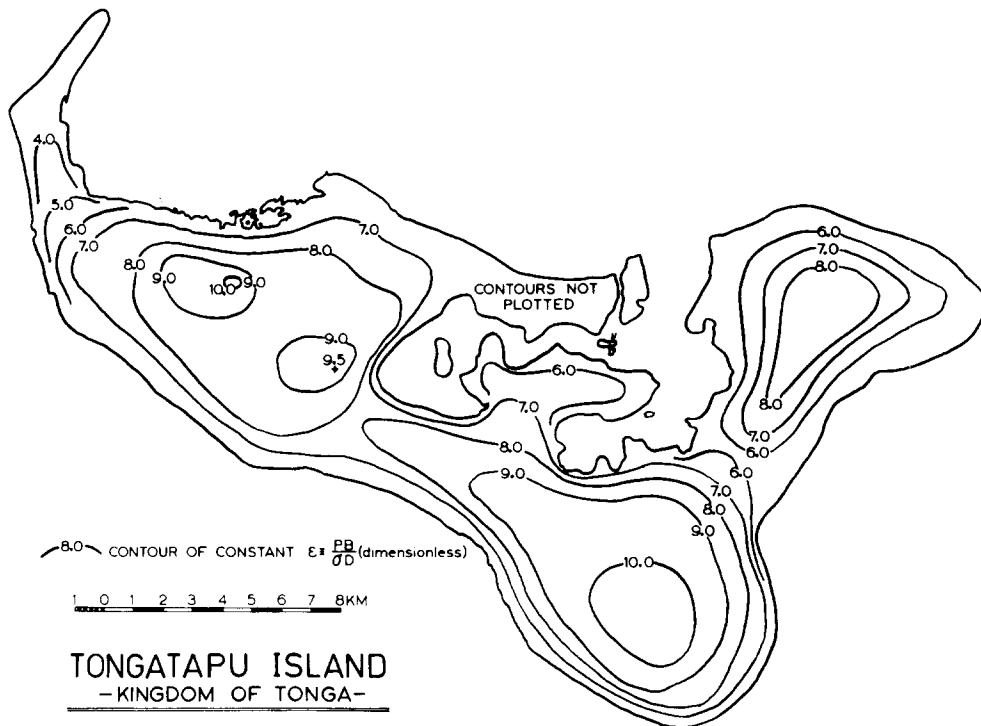One of the more interesting qualitative features of the plot in Fig. 7 is

Fig. 6. Contours of constant ϵ calculated from eq. 13.

that small changes in P, or h, create relatively large changes in Cl^- concentrations. This fact, when considered with the previously calculated result that only 25—30% of the total rainfall appears to filter through to the groundwater table, suggests that an experimental investigation into the feasibility of artificial groundwater recharge might be worthwhile. One possibility might be to induce recharge by digging pits through the topsoil in low-lying areas where rainfall tends to pond. Another possibility might be direct recharge of water through unused wells.

CONCLUSIONS

Calculations carried out herein suggest that:
(1) Thicknesses of the fresh-water lens vary from zero around the island edges to a maximum of about 20 m near central portions of the island.
(2) About 25—30% of the average rainfall of 141.7 mm/month reaches the groundwater table over much of the island.
(3) Cl^- concentrations in the aquifer are largely the result of Cl^- ions dispersing upward through the fresh-water—salt-water interface.
(4) Cl^- concentrations can be decreased in the aquifer by increasing recharge rates or decreasing abstraction rates. This will also have the effect of increasing the fresh-water lens thickness.
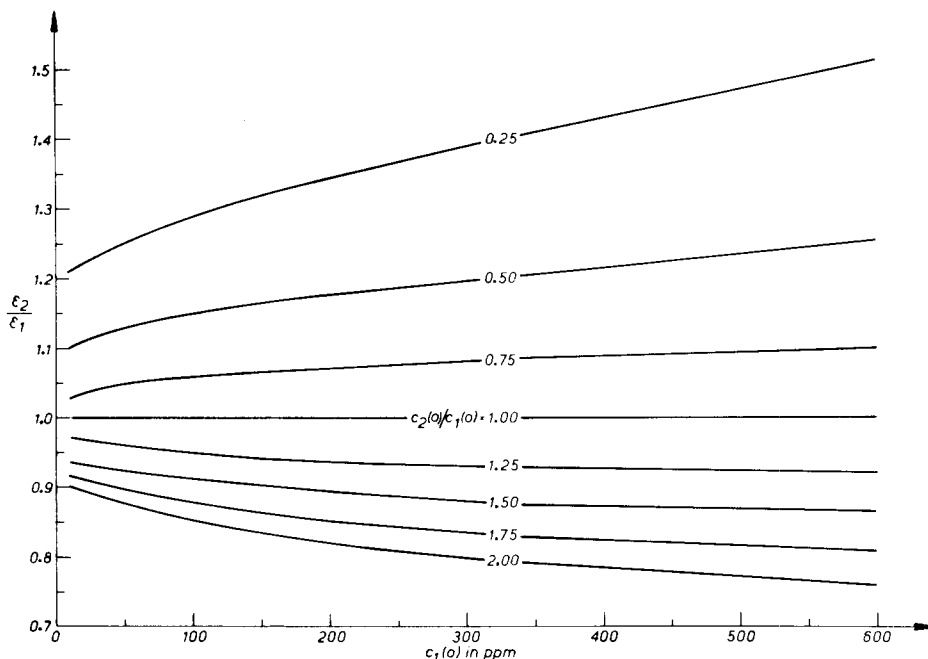
Fig. 7. A plot that can be used to estimate changes in $c(0)$ resulting from changes in either P or h.

(5) Control of Cl^- concentrations by artificial groundwater recharge may be feasible and should be investigated experimentally.

REFERENCES

Bear, J., 1972. Dynamics of Fluids in Porous Media. American Elsevier, New York, pp. 374—378; 559—560, Ch. 10.
Forbes, R.H., 1977. First report on geoelectric survey of Tongatapu Island, Kingdom of Tonga. Rep. to Tonga Water Board, Nuku'alofa, 25 pp.
Fried, J.J., 1975. Groundwater Pollution. Developments in Water Science Series, Vol. 4, Elsevier, Amsterdam, p. 312.
Harr, M.E., 1962. Groundwater and Seepage. McGraw-Hill, New York, N.Y., p. 8.

Polubarinova-Kochina, P.Ya., 1972. Theory of Ground Water Movement. Princeton
     University Press, Princeton, N.J., p. 408 (translated by J.M.R. De Wiest).
Smith, G.D., 1965. Numerical Solution of Partial Differential Equations. Oxford University
     Press, London, Ch. 5.
Waterhouse, B.C., 1976. Nuku'alofa water supply, Tonga. N.Z. Geol. Surv., Otara, Rep.,
     7 pp.